International Journal of Automotive Technology, Vol. 20, No. 5, pp. 943–948 (2019)
DOI 10.1007/s12239–019–0088–6

pISSN 1229–9138/ eISSN 1976–3832

NUMERICAL DRAG REDUCTION OF A GROUND VEHICLE BY NACA2415 AIRFOIL STRUCTURED VORTEX GENERATOR AND SPOILER

Bayindirli Cihan*

Nigde Vocational School of Technical Sciences, Nigde Omer Halisdemir University, Nigde 51000, Turkey

(Received 13 December 2018; Revised 21 February 2019; Accepted 25 February 2019)

ABSTRACT–Using of computational fluid dynamics (CFD) have big advanteges for design process components in the automotive industry. Flow structures around vehicle and drag forces can investigate in CFD without producing real size prototype vehicle. The drag force affect fuel efficiency and drivability too. In this study, the drag coefficient of 1/15 scale minibus model was minimizated by NACA 2415 airfoil structured vortex generator and front spoiler in Fluent®. Flow analyses were performed at the 5 different free stream velocities in the range of $2.8 \times 10^5 - 6.6 \times 10^5$ Reynolds numbers, where the dynamic similarity condition was provided. The drag coefficient of base minibus model was 0.415. The C_D coefficient of the model minibus was decreased 10.94 % with original designed NACA 2415 airfoil structured vortex generator in model 1. In total of 22.59 % drag reduction was obtained by designed front spoiler. The effect of this drag reduction on fuel consumption about 6 ~ 12 % at high vehicle speeds.

KEY WORDS : C_D coefficient, Minibus model, CFD, Vortex generetor, NACA2415, Front spoiler

NOMENCLATURE

A	: front surface are of bus model, m^2
C_D	: drag coefficient
F_D	: drag force, N
U_∞	: free stream velocity, m/s
Re	: reynolds number
v	: kinematic viscosity, m^2/s
ρ	: density of air, kg/m^3
CFD	: computational fluid dynamics
RNG	: renormalization-group
vg	: vortex generator

1. INTRODUCTION

The determination of air flow around of a vehicle and its effect to drag and lift forces are very important subject of study in automotive industry. High drag force reduces fuel efficiency and performance of vehicles. There are various ways to increase of vehicle porformance and decrease fuel consumption such as improving the efficiency of engine and reducing drag force. The reducing of drag force related to design of vehicle and flow controls. A lot of researches have been interested in this subject to improve of vehicle performance. Usually, flow separation on the vehicles generates high pressure based drag. High lift force can be produced as well. The drag force is influenced by the flow seperation. Rakibul Hassan *et al*. (2013) modified rear under body and exhaust gas redirected towards the rear separation zones. The drag coefficient of the car under analysis is found to be 0.323. The drag coefficient was reduced up to 22.13 % by different rear under-body modifications and up to 9.5 % by exhaust gas redirection towards region at the rear of the car. Three flow control methods were tested by Heinemann *et al*. (2012), for which steady air jets from thin slots across the rear were realized at different locations with different flow rates. Lift coefficient was reduced by more than 7 %, with relative rear axle lift reduction of about 5 %, while the drag coefficient increased by less than one 1 %. The aerodynamics characteristics of a SAE race car investigated with front spoiler, without front spoiler and with firewall vents focus by Hetawal *et al*. (2014). In that study, shape of the race car is modified by cutting out firewall and provided wing at front end. C_D of modified car is lower, compared to the standard race car. The drag coefficient of he model car is found to 0.7 which has front wing. The model car with cutting out of fire wall have drag of 0.75, whereas standard race car have Cd of 0.85. Cutting out of fire wall helps to provide space for air flow. The aerodynamics characteristics the of a Maruti Suzuki 800 investigated without using any aerodynamic devices by Pal and Singh (2016). They reduced drag coefficient average from 0.41 to 0.22. Kajiwara (2017) designed a rear wing to improve of a vehicle as aerodynamically. He determined in his study that as the attack angle of the rear wing increase, drag force increase at high vehicle speeds, and fuel

**Corresponding author*. e-mail: cbayindirli@ohu.edu.tr

consumption increase due to the big drag force. Peugeot 405 car both numerical method and in a wind tunnel by Al Saadi (2017). He found that the rear under body diffuser can reduce the drag by 6.14 % and vg devices can reduce the drag by 2.28 %. In a study by Nisugi *et al*. (2004) the drag reducition was obtained by using feedback flow control. It was stated that 21 % of power saving was achieved with this study. Altaf *et al*. (2014) improved the drag coefficient 11.1 % by elliptical flap design, 6.87 % by rectangular and 6.37 % flap and triangular flap design. Kim and Youn (2005) reduced drag force of truck 41.3 % by using roof fairing. Majdandžić *et al.* (2018) were performed flow anaylses using k-ω turbulence model in Reynolds-averaged Navier Stokes equations for a solar vehicle. Surface pressure distribution patterns indicates a favorable aerodynamic design of this vehicle.

The biggest force component on road vehicles is generally aerodynamic force. The vehicle meets the forward movement with the drive force provided by the engine. Reducing aerodynamic force is effective in engine power and therefore in fuel consumption. The aim of this study decrease of drag coefficient of a ground vehicle using passive flow control methods. The flow seperation on the minibus delayed and decreased by vortex generator and front spoiler aplication unless energy expenditure on vehicle.

2. MATERIAL AND METHOD

2.1. Methodology in CFD

This study includes the aerodynamic improvement of the model minibus used. Bayindirli and Çelik (2018) investigated flow structure of minibus model and numerically determined drag coefficient by CFD method in their study. In this study, vg and front spoiler were used as passive flow control method. The drawing data of model minibus is shown in Figure 1. The NACA2415 drawing coordinates and vg pairs were given in Figure 2.

3 pairs airfoil shaped vg mounted whoose height 5 mm on of roof area. When the flow structure of the base model is examined, it is seen that the flow seperation has occurred at this point. So negative pressure area increase around of vehicle. As the negative pressure area increase around of a vehicle, pressure based drag coefficient increase. It is intended to reduce flow speration with vortex generator pairs. The position of the vortex generator on the vehicle is given in the Figures 3 and 4.

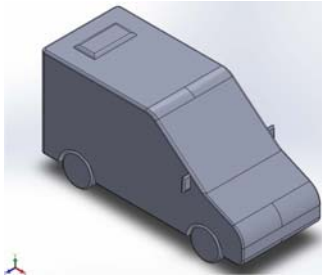

Figure 1. SolidWorks drawing of model minibus (ızometric viev) (Bayindirli and Çelik, 2018).

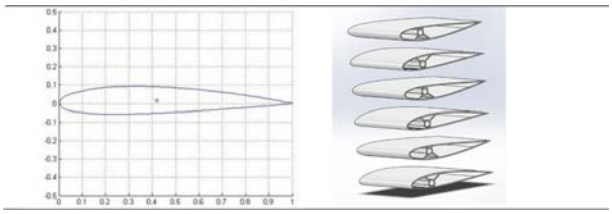

Figure 2. NACA2415 drawing coordinates and vortex genarator pairs.

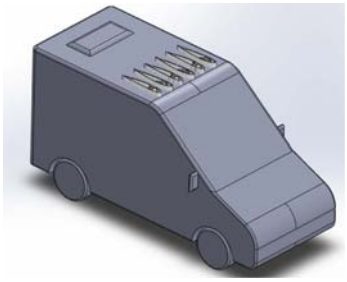

Figure 3. Model 1 minibus (ısometric view).

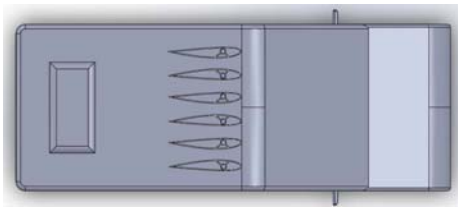

Figure 4. Model 1 minibus (top view).

To decrease flow seperation on the roof area, a front spoiler designed and mounted the minibus model. The drawing data of front spoiler and position on the minibus were given in the Figures 5 and 6.

The flow analyses were performed in Fluent® program. This CFD package program solves general integral equations for continuity, momentum, energy, turbulence based on the finite volume method.

In analyses, convergence criteria was taken 1.0×10^{-3} for continuity, x-velocity, y-velocity and z-velocity. The intensity of turbulence was 1 %. The air density was 1 kg/m^3 and the dynamic viscosity is 1.56×10^{-5}.

In flow anaylses k-ε RNG turbulence model was used. The numeric flow analysis were carrieded out using Workstation computer.

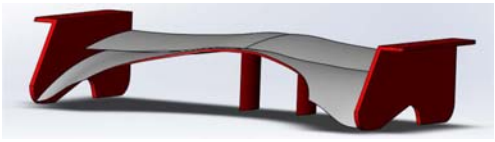

Figure 5. SolidWorks drawing of front spoiler.

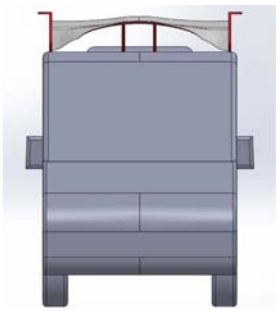

Figure 6. Model 2 minibus with front spoiler.

2.2. Similarity Conditions

In studies on vehicle aerodynamics, three different similarity conditions must be provided between prototype and model car. These are geometric, kinematic and dynamic similarity conditions. To provide geometric similarity, the licensed minibus model has been used. In kinematic similarity the rate of blockage is determinat factor. The front surface area of model bus is 0.01796 m^2; front surface area of test area is 0.3364 m^2 and a blockage rate is 5.34 %. Çengel and Cimbala (2008) recommends that blocking rate should be lower than 7.5 %. Reynolds number independence was used to provide dynamic similarity in study.

2.3. Numerical Algorithm

The solution proceeds by the following steps;

(1) Generating the geometry (car model) and domain.
(2) Generating the meshing in solution domain.
(3) Setup the pressure-based solver type, absolute velocity formulation and steady flow.
(4) Specify the properties of the fluid used such as air density and viscosity and boundary conditions.
(5) The solution method of problem is the pressure-velocity coupling simple scheme.
(6) Initialize solution and run calculations.
(7) Calculation of drag force and drag coefficient.
(8) Analyze the problem after specifying the convergence criteria and the iteration number.

2.4. Governing Equations

The following assumptions were used by the software package for the working fluid;

(1) Steady flow rate
(2) Incompressible fluid
(3) Newtonian fluid
(4) Fluid structure interaction is neglected
(5) Neglecting the heat transfer effects
(6) Neglecting the body forces
(7) K-ε model is most commonly used model in computational fluid dynamic to simulate average flow properties for the conditions of turbulent.

The Fluent package program numerically solves the general integral equations by using the finite volume method. The analyticalysolving of these equations are difficult too. The continuity equation was given in Equation (1). The continuity equation is expressed as the mass balance in the control volume in a flow.

$$\frac{\partial \rho}{\partial t} + \frac{\partial(\rho u)}{\partial x} + \frac{\partial(\rho v)}{\partial y} + \frac{\partial(\rho w)}{\partial z} = 0 \quad (1)$$

According to Newton's second law, the rate of change of the momentum of a fluid fraction is equal to the total of the forces acting on that fluid fraction. The momentum increase rate in the x, y and z directions of the unit volume of a fluid fraction is respectively expressed in terms of $\rho\frac{Du}{Dt}$, $\rho\frac{Dv}{Dt}$ $\rho\frac{Dw}{Dt}$ (İnce, 2010).

Navier - Stokes and continuity equations are also referred to as differential motion equations. When these equations are solved, some assumptions are taken and pressure and three components of velocity (x, y, z) are calculated. The most useful way to develop the finite volume method of Navier - Stokes equations;

$$\rho\frac{Du}{Dt} = -\frac{\partial p}{\partial x} + div(\mu \text{ grad } u) + S_{Mx} \quad (2)$$

$$\rho\frac{Dv}{Dt} = -\frac{\partial p}{\partial y} + div(\mu \text{ grad } v) + S_{My} \quad (3)$$

$$\rho\frac{Dw}{Dt} = -\frac{\partial p}{\partial z} + div(\mu \text{ grad } w) + S_{Mz} \quad (4)$$

2.5. Grid Strategy in CFD

The adaptive grid method was used to obtain true solution in numerical flow anayses. The objective of an adaptive grid method is to increase of solution accuracy by providing dynamic refinement. H-refinement was used to obtain better mesh quality by increasing the total number of grid elements (parent to child cells) within a base grid. This technique, known as mesh enrichment or refinement, modifies the grid at regions where worse mesh structure avaliable. Frequently, the method carries out by subdividing grid elements into smaller components. The modification of mesh resolution by changing the mesh connectivity. The simplest strategy for this type of refinement subdivides cells, while more complex procedures may insert or remove nodes (or cells) to change the overall mesh topology. In the subdivision case, every bigger cells were divided into smaller cells.

As seen in Figures 7 (a) and (b), for the model vehicles between the numbers of 1532189-3301814 tedrahedrons were formed. Dynamic refinement used in every 100 iteration. Between the numbers of 43449-35127 cells marked for refinement, 0 cells marked for coarsening at first adaptive in analyses. The boundary conditions were defined as inlet, outlet, wall and bus model in the solution domain.

The C_D coefficient is the functions of the drag force F_D, density ρ, free flow velocity V and fronteal area of vehicle and it is given in Equation (5).

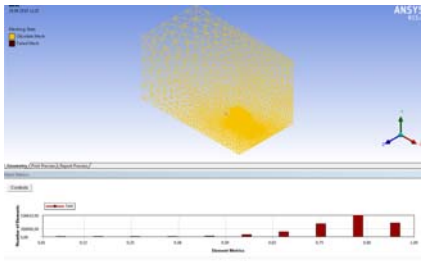

(a)

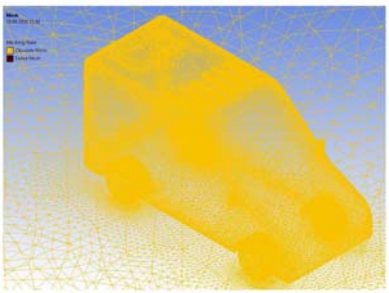

(b)

Figure 7. (a) Mesh distribution on the model 1 and mesh quality; (b) Mesh distribution on the model 1.

$$C_D = \frac{F_D}{1/2\rho V^2 A} \quad (5)$$

2.6. Mesh Independent in CFD Analysis

It is necessary to obtain a suitable and quality mesh distribution to obtain the correct results in CFD analyses. The obtaining of desired mesh quality is difficult in complex geometries. In order to achieve desired mesh quality adaptive grid refinement method was used in studies. Moreover, a grid independence study was made in order to guarantee the results does not affect from element size and quality.

In Table 1, 10 different numbers tetrahedrons grid were formed in model 1 minibus by changing mesh sizing and C_D values was determined at 25 m/s free stream velocity.

Table 1. Mesh independence test results at 25 m/s for model 1.

Reynolds number	Mesh number	C_D
472756	253125	0.25
472756	348485	0.30
472756	566021	0.31
472756	854129	0.32
472756	1191087	0.38
472756	1356347	0.38
472756	**1532189**	**0.37**
472756	1969190	0.37
472756	2361925	0.38
472756	2810146	0.37

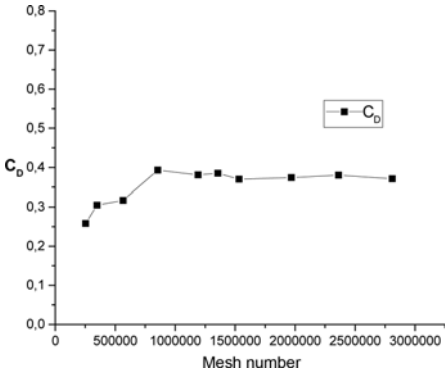

Figure 8. Graph of mesh independent.

As seen in Figure 8, the C_D coefficient was obtained at near values after 1191087 mesh numbers. 1532189 mesh number was formed for model 1 at first. It was in region where the independence was obtained. So it was took in consideration that numerical flow tests were conducted independently from mesh.

3. RESULTS AND DISCUSSIONS

3.1. Drag Reduction with Passive Flow Control Method

The C_D coefficient of the base model minibus was determined as 0.415. It was determined that 91.20 % of the total drag force was caused by pressure induced and 8.8 % by friction based (Bayindirli and Çelik, 2018). As seen in Table 2 and Figure 9, the C_D coefficient of the model minibus 1 was determined as 0.370 in same free stream velocity and Reynolds number. This results show that 10.94 % aerodynamic improvement obtained by using vortex generator. The C_D coefficient of the model 2 minibus was determined as 0.322. Average 22.59 % drag reduction obtained by using front spoiler.

The flow seperation on upper roof area decreased by vortex generator aplication in model 1. So aerodynamic drag coefficient minimizated 10.94 %. The air flow was

Table 2. Comparison of base minibus- model 1 minibus C_D coefficients.

Velocity (m/s)	Reynolds number	Base model C_D	Model 1 C_D	Model 2 C_D
15	283653	0.435	0.370	0.329
20	378205	0.433	0.370	0.316
25	472756	0.391	0.373	0.323
30	567307	0.412	0.364	0.319
35	661859	0.405	0.373	0.321
	Average	0.415	0.370	0.322
Drag reduction			10.94 %	22.59 %

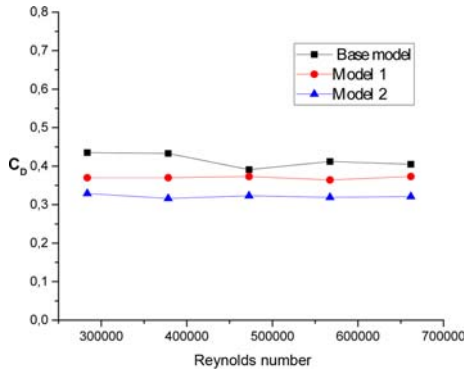

Figure 9. Comparison graph of drag coefficients.

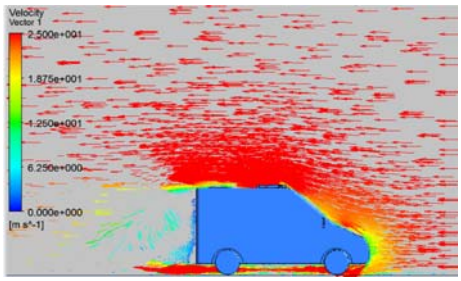

Figure 10. Vector image around of model 1 at 25 m/s velocity.

holded on the vehicle upper roof surface by positioned vortex generators pairs. Such flow seperation and negative pressure zone formation was reduced. Thanks to the minimizated negative pressure area the pressure based drag force was decreased. Flow analysis and flow visualiations showed that this passive flow control method has positive effect to drag force. The flow visuals and flow images around model 1 minibus are given in Figures 10 ~ 12.

Over the upper surface of model minibus there is a thin layer of air exists. The velocity of the air is reduces due this surface. This layer is called boundary layer. The length of the boundary layer increases as air flow drift apart from the surface. The boundary layer initially will be laminar and transforms into turbulent flows as it moves further over the larger distance. When there are sudden change in the

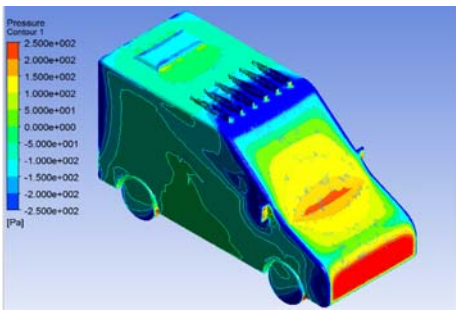

Figure 11. Pressure distribution on the model 1 at 25 m/s velocity.

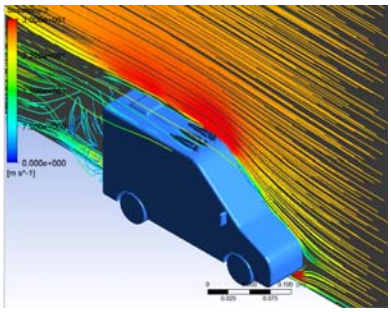

Figure 12. Streamline image around of model 1 at 25 m/s velocity.

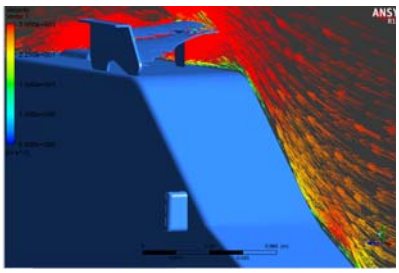

Figure 13. Vector image around of model 2 at 30 m/s velocity.

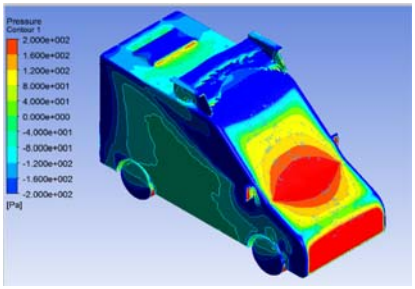

Figure 14. Pressure distribution on the model 2 at 30 m/s velocity.

surface this would lead to flow separation. Flow speration create negative pressure area and efect to vehicle along the surfce of body. As the negative pressure increases pressure based drag force increases. Using this front spoiler, air flow separation decreased and air flow was kept under control in

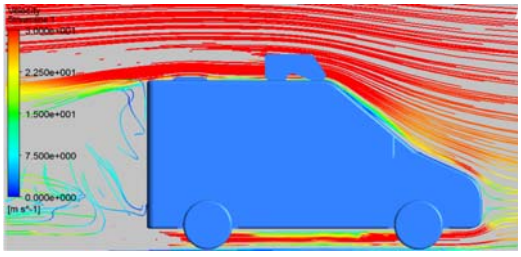

Figure 15. Streamline image around of model 2 at 30 m/s velocity.

thin boundary layer. So pressure based drag force was decreased and average 22.59 % drag reduction was obtained in model 2 by this flow control method. Flow visualiations around of model 2 minibus are given in Figures 13 ~ 15.

4. RESULT

Patil *et al*. (2012) was reduced the drag coefficient of a bus model by adding external features along with the front face adjustment. These techniques have shown about 20 ~ 30 % drag reduction can obtain on a bus. Akansu *et al*. (2016) decreased the drag coefficieint of a truck trailer model 15.71 % by using new spoiler design. They obtained 22.46 % aerodynamic improvements using passive air channel and a spoiler. The drag force of a road vehicle is responsible for a big part of the vehicle's fuel consumption and contribute up to 50 % of the total vehicle fuel consumption at high vehicle speeds. There are many scientific studies on reducing reducing aerodynamic drag of ground vehicles and increasing of their fuel efficiency. This study mainly focuses on the methods decrease of pressure based drag force and air flow separation. In this study drag coefficient of a 1/15 scale minibus model was reduced by using vortex generator and front spoiler. The drag coefficient of the base minibus model was 0.415. 10.94 % aerodynamic improvement was achieved by using airfoil structured vortex generator pairs. A front spoiler aplication was conducted on minibus model to decrease flow sereration where on roof area of minibus model. The drag coefficient of minibus model decreased average 22.59 %. The air flow is hold on roof area of vehicle by used these passive flow control method. Thus the area of the negative pressure was reduced which the vehicle was exposed. As a result of this study the aerodynamic improvement potential which can be obtained by decreasing flow separation in the upper roof area has been revealed by the CFD method. The fuel consumption of minibus model can be reduced with these techniques between the rates of 6 ~ 12 %.

REFERENCES

Akansu, Y. E., Bayindirli, C. and Seyhan, M. (2016). The improvement of drag force on a truck trailer vehicle by passive flow control methods. *J. Thermal Science and Technolog* **36**, **1**, 133–141.

Al Saadi, S. M. F. (2017). *Aerodynamic Characteristics of Peugeot 405 Car Model*. M. S. Thesis. University of Baghdad. Baghdad, Iraq.

Altaf, A., Omar, A. A. and Asrar, W. (2014). Passive drag reduction of square back road vehicles. *J. Wind Engineering Industrial Aerodyamics*, **134**, 30–43.

Bayindirli, C. and Çelik, M. (2018). The investigation of flow structure around of a minibus model by CFD method. *Proc. IV Int. Academic Resarch Cong*., Alanya, Turkey.

Çengel, Y. A. and Cimbala, J. M. (2008). *Fundamentals of Fluid Mechanics and Applications*. Güven Publish. İzmir, Turkey.

Heinemann, T., Springer, M., Lienhart, H., Kniesburges, S. and Becker, S. (2012). Active flow control on a 1/4 car model. *Proc. 16th Int. Symp. Applications of Laser Techniques to Fluid Mechanics*, Lisbon, Portugal.

Hetawal, S., Gophane, M., Ajay, B. K. and Mukkamala, Y. (2014). Aerodynamic study of formula SAE car. *Procedia Engineering*, **97**, 1198–1207.

İnce, İ. T. (2010). *Aerodynamic Analysis of GTD Model Administrative Service Vehicle*. Ph. D. Dissertation. Gazi Universty Institute of Science. Ankara, Turkey.

Kajiwara, S. (2017). Passive variable rear-wing aerodynamics of an open wheel racing car. *Automotive and Engine Technology* **2**, **1-4**, 107–117.

Kim, C. H. and Youn, C. B. (2005). Aerodynamic effect of roof fairing system on a heavy-duty truck. *Int. J. Automotive Technology* **6**, **3**, 221−227.

Majdandžić, L., Buljić, D., Buljac, S. and Kozmar, H. (2018). Aerodynamic design of a solar road vehicle. *Int. J. Automotive Technology* **19**, **6**, 949−957.

Nisugi, K., Hayase, T. and Shirai, A. (2004). Fundamental study of aerodynamic drag reduction for vehicle with feedback flow control. *JSME Int. J. Series B.* **47**, **3**, 584–592.

Pal, S. S. and Singh, A. (2016). Design and simulate an aerodynamic car body for the Maruti Suzuki 800 with less coefficient of drag. *Int. Research J. Engineering and Technology* **3**, **6**, 299–303.

Patil, C. N., Shashishekar, K. S., Balasubramanian, A. K. and Subbaramaiah, S. V. (2012). Aerodynamic study and drag coefficient optimization of passenger vehicle. *Int. J. Engineering Research and Technology* **1**, **7**, 1–9.

Rakibul, H. S. M., Islam, T., Ali, M. and Quamrul, I. M. (2013). Numerical study on aerodynamic drag reduction of racing cars. *Procedia Engineering*, **90**, 308–313.